**DOI: 10.71762/n85w-k683**

Research Paper

# Exploring the Impact of Rubber Friction in the Localized Pipe Hollowing Process Using a Rubber Pad

**Ehsan Mehrabi Gohari[1*], Iman pishkar[2], Meysam Darvishi[3]**
[1]Department of Mechanical Engineering, National University of Skills (NUS), Tehran, Iran
[2]Department of Mechanical Engineering, Payame Noor University, Tehran, Iran
[3]Specialist at Pars Oil and Gas Company
[*]Email of the Corresponding Author: emehrabi@nus.ac.ir
*Received: October, 27, 2024; Accepted: January 24, 2025*

**Abstract**
The utilization of flexible layers in the shaping of metal sheets is currently a prominently studied method. However, the efficacy of this approach depends on various parameters, including the material composition of the rubber, its thickness, frictional characteristics, and others.. This study investigated the localized diameter reduction of ST37 steel pipes using a rubber ring. We employed both experimental and numerical methods, utilizing finite element analysis (FEA) to explore the influence of friction between the rubber and the metal. Experiments were conducted to validate the FEA models. Subsequently, simulations were performed with varying friction coefficients at the rubber-metal interface. The results were analyzed graphically to understand the impact of friction on the diameter contraction process. Our findings provided insights into the critical role of friction in this shaping technique and offered recommendations for optimizing the process.

**Keywords**
Rubber Pad, Localized Diameter Hollowing, Finite Element Method, Friction Coefficient, Friction Force

## 1. Introduction

In conventional methods of metal sheet forming, a mandrel and rigid metal matrix are employed to shape the raw sheet. In recent years, there has been a notable emphasis on employing rubber layers to exert force on the sheet. This approach shapes a diverse array of components within the aviation industry. The advantages of using this method include reducing mold-making costs, minimizing the possibility of creasing, and improving the surface quality of the final product. Factors such as the limited lifespan of rubber or high energy consumption can be considered drawbacks of employing this method [1-4]. In numerous industrial applications today, finite element methods simulate the process. In metal sheet forming, simulation serves as a tool to forecast the behavior of raw materials and manage factors such as creasing and tearing in the initial piece. However, a significant limitation in process simulation is the software's inability to accurately model friction distribution in the contact areas between the piece and the tool. Frictional behavior depends on several parameters, including

the pressure between contact surfaces, sliding speed of the surfaces, materials of the part and mold, surface coarseness, lubrication level between surfaces, and the type of deformation (considering symmetry aspects). The friction sensitivity in applications like forming with flexible tools, where contact points are more complex, becomes notably pronounced [5-7]. In recent years, numerous studies conducted by various researchers have focused on investigating the impact of friction in forming methods involving flexible tools. Browne and Battikha conducted valuable experimental tests using a rubber pad to evaluate the forming process [8].

In this research, the investigation involved repeating the process with various lubricants applied to the contact surfaces of the samples to study the occurrence of creasing and tearing in parts with different materials. Also, Deladi [9] investigated the impact of friction in the forming method employing rubber pad, aiming to advance the fundamental principles of stationary static in this context. Subsequently, Felhos et al. [10] conducted both experimental and numerical investigations into the friction behavior of a steel ball rolling on a rubber plate. In this study, both normal and tangential forces were taken into account during the measurements. Ramezani et al. [11] employed experimental and numerical methods to study the stamping process. Additionally, they examined the effects of parameters such as rubber material and hardness, process speed, rubber thickness, and friction on the quality of the process. In another study, Ramezani et al. [12] examined the effect of friction in pipe bulging using flexible tools. In this research, theoretical models were employed to evaluate the static friction at the interface between the rubber and the pipe. Subsequently, numerical analysis of the process was conducted. In 2009, in another study, Ramezani et al. [13] theoretically examined the influence of friction. They subsequently conducted numerical and experimental investigations on the effects of both static and dynamic friction in forming an incomplete cone. Balcerzak et al. [14] presented the results of numerical simulations and experimental tests of plastic forming sheets made from the difficult-to-deform nickel alloy Inconel 718 with a thickness of 1 mm. They found that one of the important aspects of plastic forming sheets using the Guerin method is the tendency to obtain a diversified shape of the final elements. Esmailian [15], in a research, he simulated and optimized the nosing forming process of metal pipes with the help of genetic algorithm. In 2023, a new flexible multi-point incremental sheet forming process with multi-layer sheets (F-MPIF-MLS) was proposed by Xuelei and Hengan [16]. Their results showed a noticeable reduction of wrinkling by using the new flexible multi-point die over the conventional multi-point die system with multi-layer sheets to form a dome shape.

This study begins with exploring the experimental and numerical investigation of pipe hollowing using rubber tools. Subsequently, it validates the numerical findings through comparison with experimental results and numerically examines the effect of friction. Efficiency and pressing force under varying friction conditions are analyzed using diagrams. Finally, based on the results obtained, the role of friction and strategies for its adjustment are investigated.

## 2. Introduction of the examined piece and mold

The research focuses on a tested sample comprising a st37 steel pipe. This sample features an inner diameter of 144.9 mm a thickness of 2 mm, and stands at a height of 73.4 mm. The objective is to achieve a diagonal reduction of 12 mm and a height reduction of 24 mm at the midpoint of the piece.

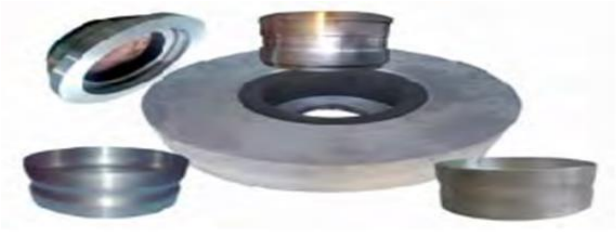

Figure 1. Schematic depiction of the mold and its components alongside two fabricated samples.

A rubber cylinder is placed behind the piece to create a groove, which is externally constrained by a container to prevent unintended deformations. Moreover, a matrix to fit the desired groove is placed inside the pipe. A mandrel is utilized to employ pressing force on the rubber. The mandrel presses the rubber layer, and the lateral strain of the rubber is utilized to alter the shape of the workpiece.

## 3. Governing relationships on problems

Because of their unique physical properties, elastomers and rubbers exhibit different characteristics than other materials. These materials, capable of large elastic deformations, are called super elastic materials. Some of these materials, like rubbers, experience a slight decrease in volume under high strain. Therefore, they are often categorized as incompressible materials.

In finite element software, various material models employing different forms of strain energy potential are utilized to analyze the behavior of incompressible superelastic materials. Among these models, the Mooney-Rivlin model is renowned as a prominent structural model for superelastic materials, particularly in incompressible natural rubber. This model includes four models compromising 9-parameter, 5-parameter, 3-parameter and 3-parameter states. The strain potential energy for the 2-parameter state is given as follows [16]:

$$W = c_{10}\,(I1 - 3) + c_{01}\,(I_2 - 3) \frac{1}{d}\,(J - 1)^2 \quad (1)$$

Where $c_{10}$ and $c_{01}$ represent material constants, the initial bulk modulus is also determined using the following relationships.

$$K = \frac{2}{d} \quad (2)$$

$$K = \frac{2(c_{10} + c_{01})}{(1 - 2v)} \quad (3)$$

## 4. Simulating the finite elements of the process

Ansys, the finite element software utilized in this research, models the process. The model's symmetry is exploited to simplify the problem-solving process, and the simulation is in axial symmetry mode. This section introduces the fundamental parameters considered in the simulation.

### *4.1 The Utilized elements*

The Hyper56 element is utilized for simulating the rubber, as it adheres to the behavioral characteristics of Mooney-Rivlin materials. The Plane42 element is also utilized to grid the tested sample, matrix, and container.

*4.2 Introduction of the materials*

To define the material model of steel, after specifying its linear behavior, the Bilinear Isotropic Hardening model is used to describe its non-linear behavior in the plastic region. In this model, the material behavior is represented by two straight lines on the stress-strain curve: the slope of the first line is the modulus of elasticity (E), and the slope of the second line is the tangential slope ($E_t$) [17]. The sample is made of st37 steel. The specifications of this steel are presented in Table 1.

Table 1. The specifications of st37 steel [18]

| **E(GPa)** | $\boldsymbol{\sigma_y(MPa)}$ | $\boldsymbol{\sigma_u(MPa)}$ | **v** |
|---|---|---|---|
| **210** | 245 | 410 | 0/27 |

The rubber used in the test is commonly found in tractor tires, with a hardness of 70 Shore [19]. The physical characteristics of this rubber are detailed in Table 2.

Table 2. Characteristics of the rubber used in the process [18]

| **E(MPa)** | $\boldsymbol{c_{01}(MPa)}$ | $\boldsymbol{c_{10}(MPa)}$ |
|---|---|---|
| **10** | 1/805 | 0/8061 |

*4.3 Calculation of Poisson's Coefficient*

The bulk modulus and deformation coefficients are utilized to calculate Poisson's coefficient for rubber. Additionally, the related relations are:

$$P = k.e \quad (4)$$

$$P = \sigma_x + \sigma_y + \sigma_z \text{ And } e = \varepsilon_x + \varepsilon_y + \varepsilon_z \quad (5)$$

To calibrate v, according to equation 4, the rubber is placed in a container, a specific pressure is applied, and the resulting strain is measured. From these measurements, the bulk modulus is calculated. By inserting this value into equation 3, Poisson's ratio is determined to be 0.495.

*4.4 Loading*

After defining the contact elements, the necessary loading must be applied, and the problem must be solved. The required loadings for this process include defining the line of axial symmetry, constraining the nodes of the matrix and container in all directions, and displacing the upper nodes of the rubber in the Y direction.

*4.5 Problem solver settings*

In the process of shaping with a rubber pad, numerous factors contribute to the non-linearity of the analysis. Significant deformations in the metal and rubber, non-linear material models, and extensive contact surfaces increase the computational requirements.

## 5. Experimental testing and validation of numerical results

In this section, the experimental investigation of the process is conducted based on the results obtained from the numerical solution. Efforts are made to minimize factors that may adversely affect the process during testing to ensure accurate results. These factors include friction, misalignment of mold and press components, and methods of applying force. Figure 2 compares the formed pieces with the simulated piece after undergoing shape modification.

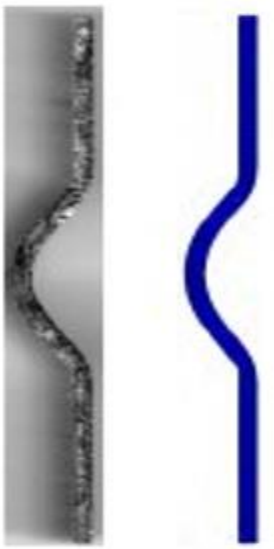

Figure 2. Experimental comparison of 6 mm grooved steel profile with numerical results

After the test, a notable observation is the absence of wrinkles in the final piece. This condition can primarily be attributed to the rubber's role in preventing the piece's folding or wrinkling piece. This behavior can be attributed to two primary reasons. Firstly, the rubber acts as a sheet gripper by exerting pressure on the piece, thereby controlling the sheet's flow. Secondly, as pressure increases, the rubber's surface hardens, exerting pressure on the deforming area from the back of the piece and preventing the formation of wrinkles. This phenomenon is considered a beneficial outcome of this process. To ensure accurate verification of these results, both experimentally and numerically, deformation curves of the internal and external surfaces of the sample are compared using both methods. Figures 3 and 4 illustrate this comparison.

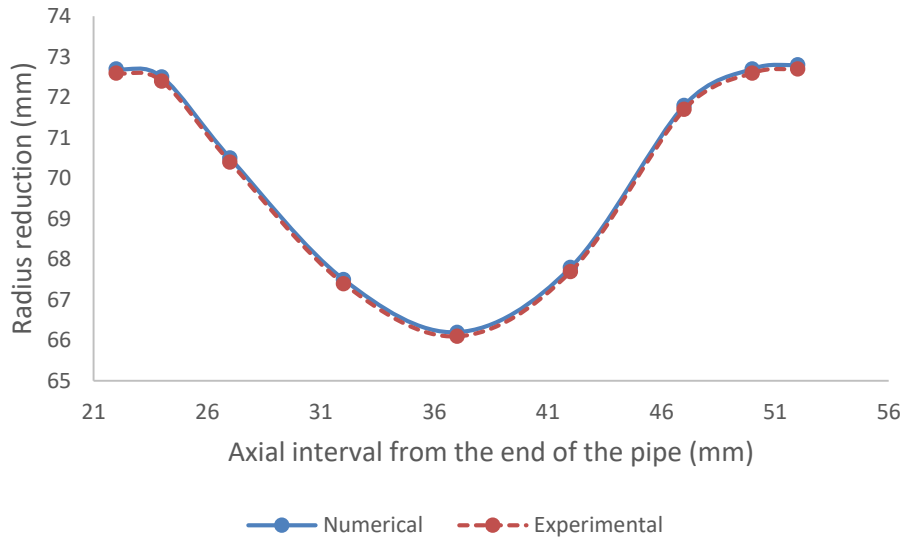


Figure 3. Radius change curve on the internal surface of the sample with a 6 mm groove: numerical and experimental comparison

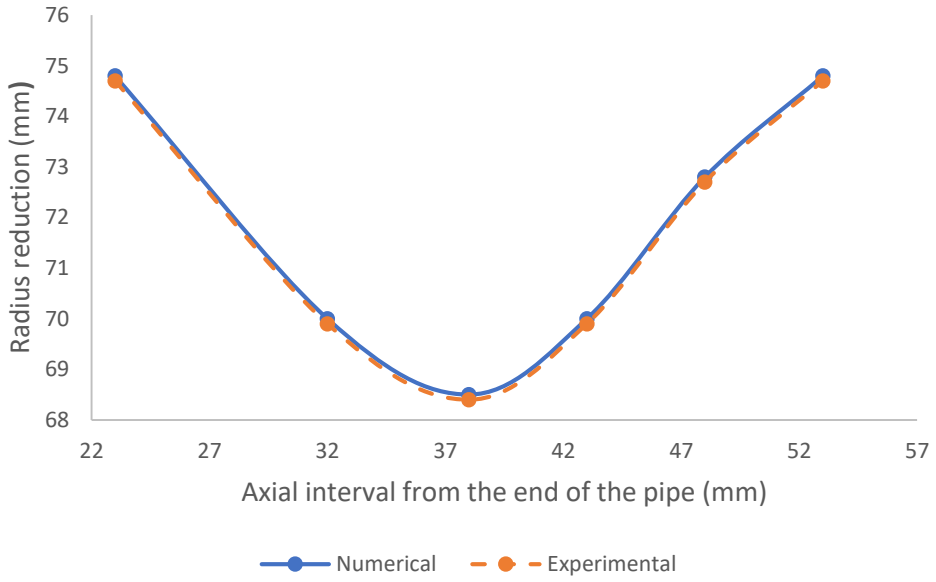


Figure 4. Radius change curve on the external surface of the sample with a 6 mm groove: numerical and experimental comparison

## 6. Investigating the impact of friction variation

Following the successful alignment observed between experimental and numerical investigations of the pipe hollowing process in the previous section, this section delves into the impact of friction within this process. This process encounters two types of friction: one between the pipe and the matrix and the other between the rubber and the metal. In this study, the focus is on evaluating the impact of friction between rubber and metal. Simulations are conducted multiple times to assess this effect, using various static friction coefficients, and the results are subsequently graphically presented. In the first diagram, the efficiency of each test is analyzed. This efficiency is defined as the ratio of the

plastic work performed on the steel pipe to the total energy applied by the press. The initial observation from the results is the variation in the displacement required by the mandrel to make the first contact between the pipe's inner surface and the groove's bottom. Figure 5 illustrates the displacement of the mandrel at the point of contact between the matrix's inner surface and the groove's bottom for each friction factor.

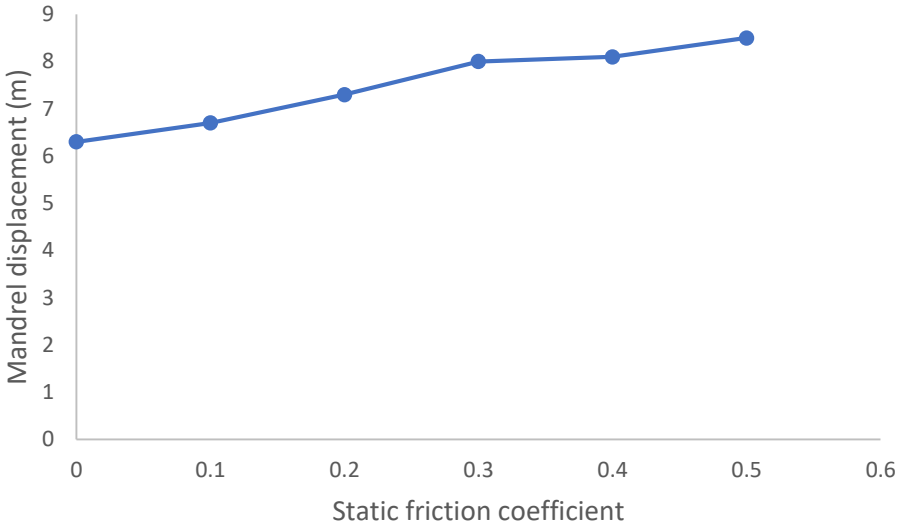


Figure 5. Mandrel displacement at the initial contact between the pipe and the bottom of the groove

The diagram shows that the mandrel displacement required to achieve the desired shape change on the sample increases as the friction coefficient increases. Figure 6 examines the amount of pressing force used in each simulation.

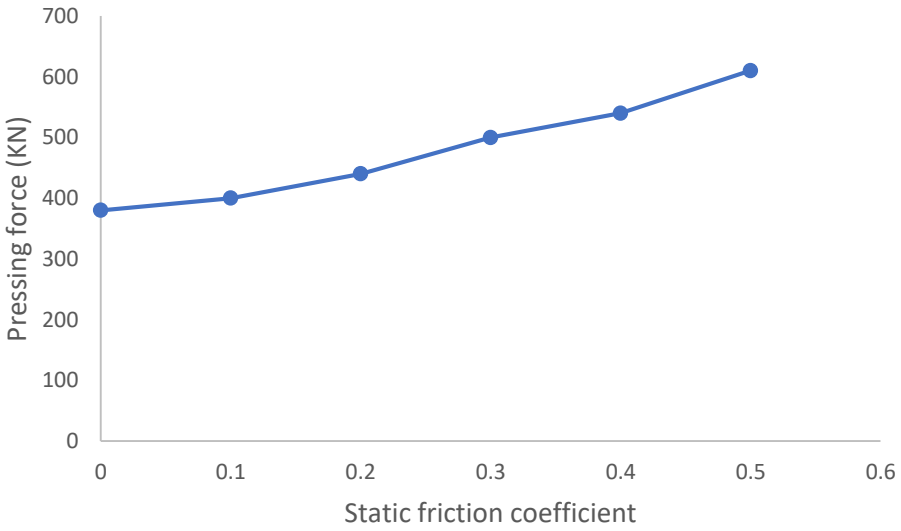


Figure 6. Pressing force curve according to the various friction coefficients

The diagram shows that the pressing force increases in parallel with the friction coefficient. Figure 7 presents the efficiency of the process calculated in each experiment and included in the chart.

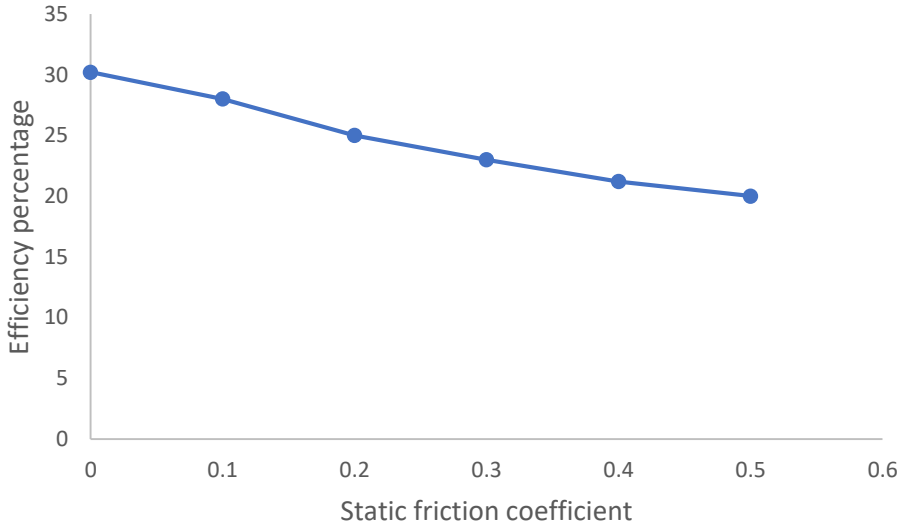


Figure 7. Efficiency curve according to the various friction coefficients

## 7. Interpretation of the results

As evident from the diagrams in the previous section, the friction coefficient can be identified as a fundamental parameter in the process of localized pipe hollowing.

In this process, it is evident that on both the inner and outer surfaces of the rubber in contact with the metal, the friction force prevents the movement of the rubber along the axis. As the rubber is compressed further due to increased pressure between the rubber and the metal, the intensity of this resistance force increases. Therefore, the axial force required to create the desired movement in the rubber increases. This mode explains the increase in pressing force observed in Figure 6, which, in turn, necessitates a more significant displacement of the mandrel. Another crucial aspect is the friction coefficient's impact on the process's efficiency. Increasing the friction coefficient necessitates more energy to overcome frictional resistance. Moreover, higher friction leads to increased pressing force and mandrel displacement. These factors collectively demand more excellent compressibility of the rubber. Therefore, another portion of the pressing energy is expended on compressing the rubber. Consequently, considering these factors and the nearly constant amount of practical plastic work performed on the pipe across different friction coefficients, the process efficiency decreases with increasing friction.

## 8. Conclusion

As observed, an increase in the coefficient of friction augments the resistive force, leading to a higher pressing force and reduced process efficiency. Consequently, based on the above findings, reducing friction enhances the process. To address this issue, improving the quality of contact surfaces and decreasing the roughness of metal surfaces at contact points can be effective. Additionally, employing lubricants and thin layers with high surface smoothness can help to mitigate friction.

Based on the conducted research, the following general conclusions can be drawn:

1. Increasing the friction coefficient increases the pressing force.
2. Increasing the friction coefficient increases the displacement of the mandrel.
3. Increasing the friction coefficient decreases the efficiency of the process.
4. Increasing the friction coefficient increases erosion on the rubber surfaces.
5. Increasing the friction coefficient results in less height reduction of the sample after the process.
6. Increasing the friction coefficient leads to greater sample thickness in the area under deformation after the process.

## 9. References

[1] Hagenah, H., Schulte, R., Vogel, M., Hermann, J., Scharrer, H., Lechner, M. and Merklein, M. 2019. 4.0 in metal forming - questions and challenges.79(1):649–654. doi:10.1016/j.procir.2019.02.055.

[2] Gronostajski, Z., Pater, Z.; Madej, L., Gontarz, A., Lisiecki, L., Lukaszek-Solek, A., Luksza, J., Mróz, S., Muskalski, Z. and Muzykiewicz, W. 2019. Recent development trends in metal forming. Arch. Civ. Mech. Eng. 19(1):898–941. doi:10.1016/j.acme.2019.04.005.

[3] Trzepieciński, T. 2020. Recent Developments and Trends in Sheet Metal Forming. Metals. 10(1): 779. doi:10.3390/met10060779.

[4] Wang, P.Y., Wang, Z.J., Xiang, N. and, Li, Z.X. 2020.Investigation on changing loading path in sheet metal forming by applying a property-adjustable flexible-die. J. Manuf. Process. 53(1): 364–375. doi:10.1016/j.jmapro.2020.03.033.

[5] Andersson, Alf. 2004. Comparison of sheet-metal-forming simulation and try-out tools in the design of a forming tool. Journal of Engineering Design. 15(1): 551-561. doi:10.1080/09544820410001697598.

[6] Erfanian, M and Hashemi, R. 2018. A comparative study of the extended forming limit diagrams considering strain path, through-thickness normal and shear stress. International Journal of Mechanical Sciences. 148(1): 316-326. doi: 10.1016/j.ijmecsci.2018.09.005.

[7] Scheidl, J. and Vetyukov, Y. 2023.Review and perspectives in applied mechanics of axially moving flexible structures. Acta Mech. 234(1): 1331–1364. doi:10.1007/s00707-023-03514-5.

[8] Browne, DJ. and Battikha, E.1995. Optimization of aluminum sheet forming using a flexible die. J. Mater. Process. Technol. 55(1): 218-223. doi:10.1016/0924-0136(95)02009-8.

[9] Deladi, E.L. 2006.Static Friction in Rubber-Metal Contacts with Application to Rubber Pad Forming Processes. University of Twente. PhD thesis.

[10] Felhos, D., Xu, D., Schlarb, A. K., Varadi, K. and Goda, T. 2008.Viscoelastic characterization of an EPDM rubber and finite element simulation of its dry rolling friction XPRESS Polymer Letters. 2(3): 157-164. doi: 10.3144/expresspolymlett.2008.21.

[11] Ramezani, M., Ripin, M., MAlmad, Z. and RAkil, H. 2009. Numerical simulation of sheet stamping process using flexible punch.Journal of Engineering Manufacture. 223(7): 829-840. doi:10.1243/09544054JEM1453.

[12] Ramezani, M., Ripin, Z.M. and Roslan, A. 2009.A static friction model for tube bulge forming using a solid bulging medium. Int J Adv Manuf Technol. 43(1):238-247. doi:10.1007/s00170-008-1708-x.

[13] Ramezani, M., Ripin, Z.M. and Roslan, A. 2009.Computer aided modelling of friction in rubber-pad forming process. Journal of Materials Processing Technology. 209(1): 4925- 4934. doi:10.1016/J.JMATPROTEC.2009.01.015.

[14] Balcerzak, M., Rusz, S., Čada, R., Pastrňák, M., Hilšer, O., and Greger, M. 2024. An Investigation into Sheet-Inconel 718 Forming with Flexible and Metal Tools—Simulation and Experiment. Materials. 17(1): 3168. doi:10.3390/ma17133168.

[15] Ismailian, M. 2022. Optimization of metal pipe nosing process using genetic algorithm. Mechanics of Advanced and Smart Materials journal. 2(2): 188-201. doi: 10.52547/masm.2.2.188.

[16] Xuelei, Zh., and Hengan, O. 2023.A new flexible multi-point incremental sheet forming process with multi-layer sheets. Journal of Materials Processing Technology. 322(1):118214. doi: 10.1016/j.jmatprotec.118214.

[17] ANSYS Theory Manual for Release 5.6,1999. 11th Edition, ANSYS Inc.

[18] Papadakis L.2008. Simulation of the Structural Effects of Welded Frame Assemblies in Manufacturing Process Chains. Herbert Utz Verlag.

[19] Mohsenimanesh, A., Ward. S.M., and Gilchrist. M.D. 2009. Stress analysis of a multi-laminated tractor tyre using non-linear 3D finite element analysis. Materials & Design. 30(4):1124-32. doi: 10.1016/j.matdes.2008.06.040.